Supplemental Information

Localization of a TORC1-eIF4F translation complex during CD8$^+$ T cell activation drives divergent cell fate

Swantje Liedmann, Xueyan Liu, Clifford S. Guy, Jeremy Chase Crawford, Diego A. Rodriguez, Duygu Kuzuoğlu-Öztürk, Ao Guo, Katherine C. Verbist, Jamshid Temirov, Mark J. Chen, Davide Ruggero, Hui Zhang, Paul G. Thomas, Douglas R. Green

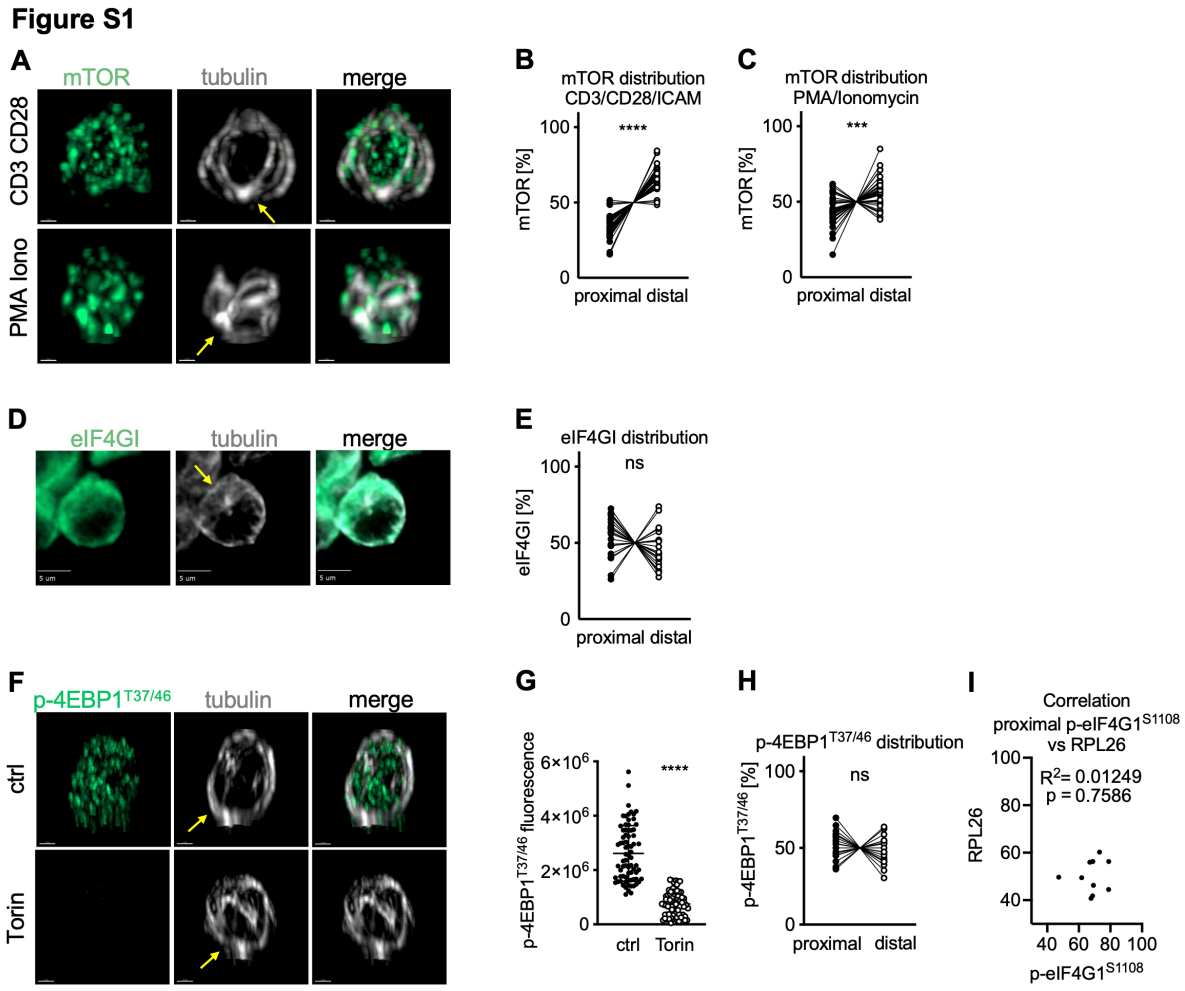

Figure S1. TORC1 signaling is localized at the proximal pole of activated, undivided OT-I CD8$^+$ T cells regulating asymmetric c-Myc synthesis. Related to Figure 1.

(**A**) Representative images of undivided OT-I CD8$^+$ T cells activated on slides coated with anti-CD3, anti-CD28, and ICAM1 or with PMA plus Ionomycin for 2 h. Scale bar: 2 µm. (**B**, **C**) Quantification of the distribution of mTOR within the cell. Each dot represents signal in the proximal or distal half of a cell. A line connects data points from two halves of the same cell. (**D**) Representative images of undivided OT-I CD8$^+$ T cells activated on peptide-pulsed APCs. Scale bar: 5 µm. (**E**) Quantification of the distribution of eIF4GI signal within the cell. Each dot represents signal in the proximal or distal half of a cell. A line connects data points from two halves of the same cell. (**F**) Representative images of undivided OT-I CD8$^+$ T cells activated on antibody-coated slides as in (A) for 2 h and treated with Torin for the last hour of activation. Scale bar: 5 µm. (**G**) Quantification of sum fluorescence intensity of p-4EBP1$^{T37/46}$. Each dot represents one cell; mean +/- SD. (**H**) Quantification of the distribution of p-4EBP1$^{T37/46}$ signal within the cell. Each dot represents signal in the proximal or distal half of a cell. A line connects data points from two halves of the same cell. (**I**) Relation between proportion of proximal p-eIF4GI^{S1108} and proximal RPL26 within the same cell by Poisson regression. Each dot represents one cell. Arrows indicate MTOCs. Compiled from two (**G**, **H**) or three independent experiments (**B**, **C**, **E**). Significance was calculated with paired (**B**, **C**, **E**, **H**) or unpaired (**G**) *Student's t-test*; ***p<0.001, ****p<0.0001, ns=not statistically significant.

Figure S2

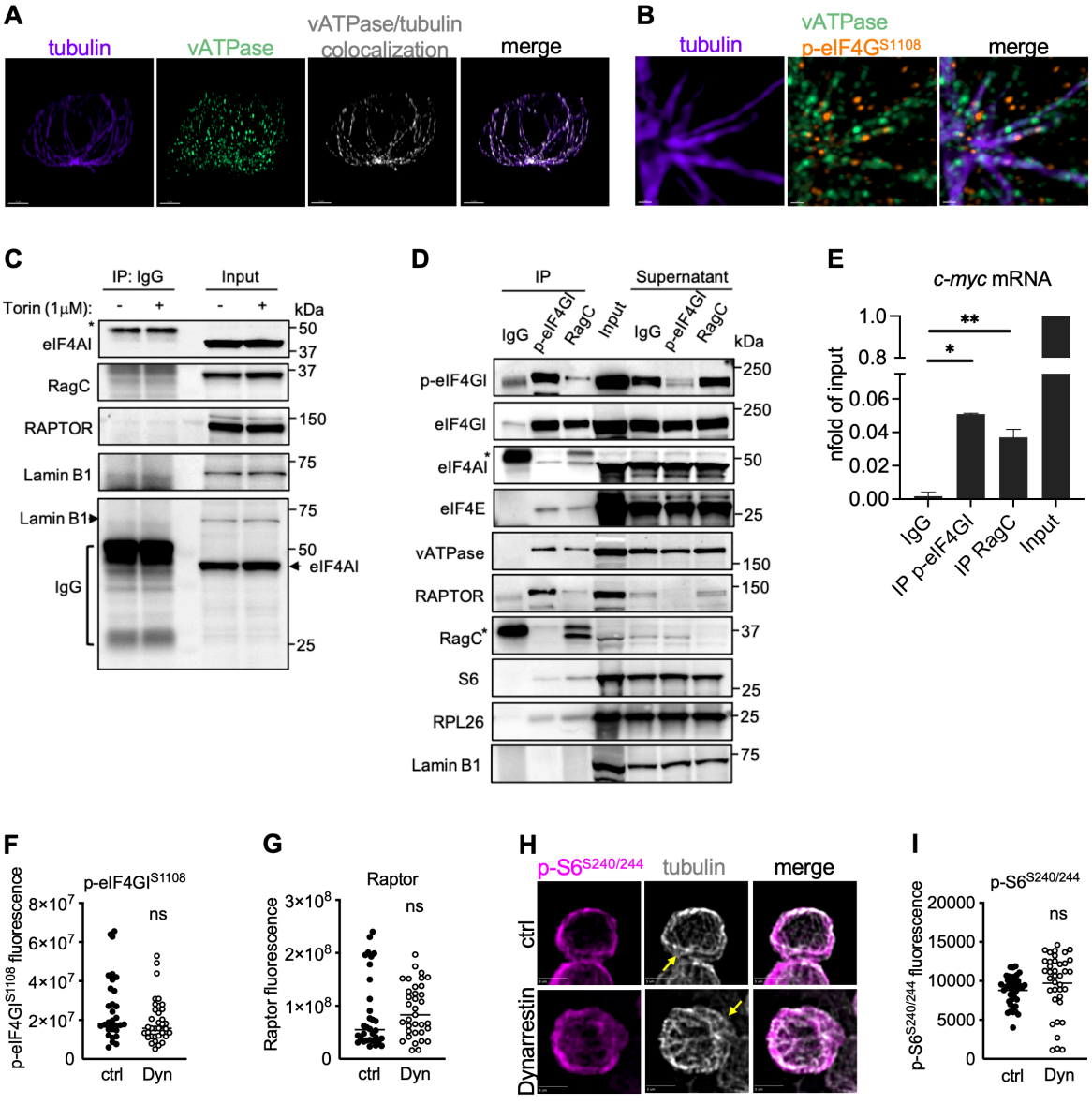
A
tubulin
vATPase
vATPase/tubulin colocalization
merge
B
tubulin
vATPase p-eIF4G^{S1108}
merge
C
IP: IgG
Input
Torin (1μM): - + - +
kDa
eIF4AI*
RagC
RAPTOR
Lamin B1
Lamin B1
IgG
eIF4AI
50
37
37
150
75
75
50
25
D
IP
Supernatant
IgG
p-eIF4GI
RagC
Input
IgG
p-eIF4GI
RagC
kDa
p-eIF4GI
eIF4GI
eIF4AI*
eIF4E
vATPase
RAPTOR
RagC*
S6
RPL26
Lamin B1
250
250
50
25
150
150
37
25
25
75
E
c-myc mRNA
nfold of input
1.0
0.8
0.06
0.04
0.02
0.00
**
*
IgG
IP p-eIF4GI
IP RagC
Input
F
p-eIF4GI^{S1108}
p-eIF4GI^{S1108} fluorescence
8×10^7
6×10^7
4×10^7
2×10^7
0
ns
ctrl
Dyn
G
Raptor
Raptor fluorescence
3×10^8
2×10^8
1×10^8
0
ns
ctrl
Dyn
H
p-S6$^{S240/244}$
tubulin
merge
ctrl
Dynarrestin
I
p-S6$^{S240/244}$
p-S6$^{S240/244}$ fluorescence
20000
15000
10000
5000
0
ns
ctrl
Dyn

Figure S2. Dynein-dependent vesicular transport mediates polarization of the TORC1-eIF4F complex towards the proximal pole of activated, undivided OT-I CD8$^+$ T cells. Related to Figure 2.

OT-I CD8$^+$ T cells activated on antibody-coated plates as in Figure S1A (A, B) or peptide-pulsed APCs (C-I). (**A**) Association of vATPase$^+$ vesicular structures along microtubules in visualized by expansion microscopy. Scale bar: 5 µm. (**B**) Association of p-eIF4GI^{S1108} with vATPase$^+$ vesicular structures along microtubules visualized by expansion microscopy. Scale bar: 1 µm. (**C**) Input control and Co-Immunoprecipitation of IgG in OT-I CD8$^+$ T cells activated on APCs for 24 h and treated with Torin for the last hour of activation. Corresponding controls to Fig. 2D. (**D**, **E**) Co-Immunoprecipitation of p-eIF4GI^{S1108} and RagC in OT-I CD8$^+$ T cells activated on APCs for 24 h. Representative Western blot (**D**) and detection of *c-myc* mRNA in IP fractions by qPCR (**E**). An asterisk indicates unspecific antibody binding. (**F**, **G**) Quantification of sum fluorescence intensity of p-eIF4GI^{S1108} (**F**) and Raptor (**G**). Each dot represents one cell; mean +/- SD. Corresponding to Fig. 2F. (**H**) Representative images of undivided OT-I CD8$^+$ T cells activated on peptide-pulsed APCs for 24 h and treated with Dynarrestin for the last hour of activation. Scale bar: 5 µm. (**I**) Quantification of sum fluorescence intensity of p-S6$^{S240/244}$. Each dot represents one cell; mean +/- SD. Arrows mark MTOCs. Compiled from two (**E**) or three independent experiments (**F**, **G**, **I**). Significance was calculated with unpaired (**E**-**G, I**) *Student's t-test*. *p<0.05, **p<0.01, ns=not statistically significant.

Figure S3

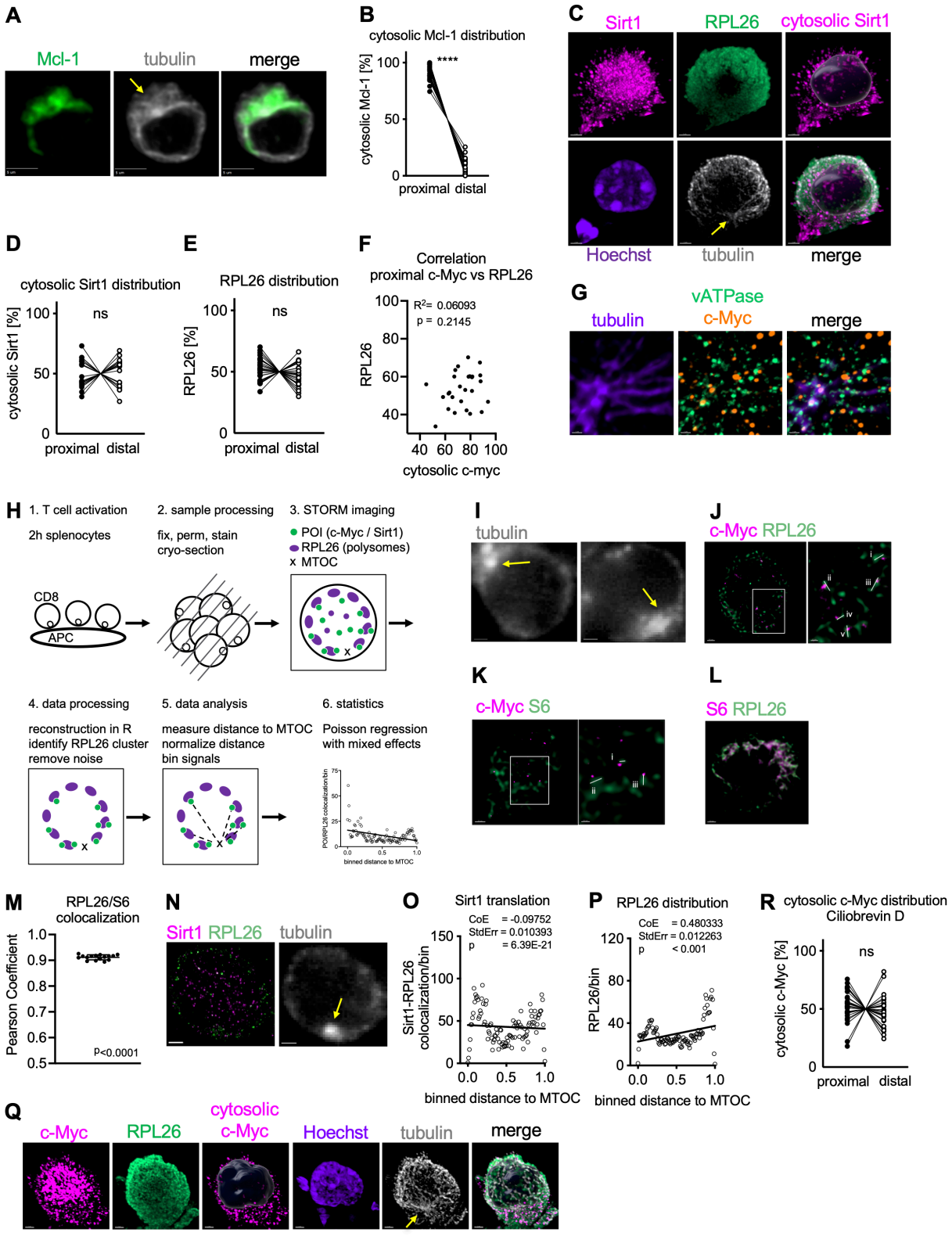
A
Mcl-1
tubulin
merge
B
cytosolic Mcl-1 distribution
cytosolic Mcl-1 [%]
****
proximal distal
C
Sirt1
RPL26
cytosolic Sirt1
Hoechst
tubulin
merge
D
cytosolic Sirt1 distribution
cytosolic Sirt1 [%]
ns
proximal distal
E
RPL26 distribution
RPL26 [%]
ns
proximal distal
F
Correlation
proximal c-Myc vs RPL26
R²= 0.06093
p = 0.2145
RPL26
cytosolic c-myc
G
tubulin
vATPase
c-Myc
merge
H
1. T cell activation
2h splenocytes
2. sample processing
fix, perm, stain
cryo-section
3. STORM imaging
POI (c-Myc / Sirt1)
RPL26 (polysomes)
x MTOC
CD8
APC
4. data processing
reconstruction in R
identify RPL26 cluster
remove noise
5. data analysis
measure distance to MTOC
normalize distance
bin signals
6. statistics
Poisson regression
with mixed effects
POI/RPL26 colocalization/bin
binned distance to MTOC
I
tubulin
J
c-Myc RPL26
K
c-Myc S6
L
S6 RPL26
M
RPL26/S6
colocalization
Pearson Coefficient
p<0.0001
N
Sirt1 RPL26
tubulin
O
Sirt1 translation
CoE = -0.09752
StdErr = 0.010393
p = 6.39E-21
Sirt1-RPL26 colocalization/bin
binned distance to MTOC
P
RPL26 distribution
CoE = 0.480333
StdErr = 0.012263
p < 0.001
RPL26/bin
binned distance to MTOC
R
cytosolic c-Myc distribution
Ciliobrevin D
cytosolic c-Myc [%]
ns
proximal distal
Q
c-Myc
RPL26
cytosolic c-Myc
Hoechst
tubulin
merge

Figure S3. C-Myc synthesis localizes to the proximal pole of activated OT-I CD8$^+$ T cells prior to the first division. Related to Figure 3.

(**A**) Representative images of undivided OT-I CD8$^+$ T cells activated on peptide-pulsed APCs. Scale bar: 5 µm. (**B**) Quantification of the distribution of Mcl-1 signal within the cell. Each dot represents signal in the proximal or distal half of a cell. A line connects data points from two halves of the same cell. (**C**-**E**) Spatial distribution of cytosolic Sirt1 in undivided OT-I CD8$^+$ T cells activated on peptide-pulsed APCs using SoRa imaging. Representative image, cytosolic Sirt1 is visualized by masking nuclear c-Myc based on Hoechst (**C**). Scale bar: 2 µm. Quantification of the distribution of cytosolic Sirt1 (**D**) and total RPL26 (**E**) within the cell. Each dot represents signal in the proximal or distal half of a cell. A line connects data points from two halves of the same cell. (**F**) Relation between proportion of proximal c-Myc and proximal RPL26 within the same cell by Poisson regression. Each dot represents one cell. (**G**) Association of c-Myc with vATPase$^+$ vesicular structures along microtubules visualized by expansion microscopy. Scale bar: 1 µm. (**H**) Experimental and analytical approaches to assess spatial distribution of c-Myc synthesis in undivided OT-I CD8$^+$ T cells by STORM. (**I**) Tubulin staining corresponding to STORM data in Fig. 3C (left) and 3D (right). (**J**, **K**) Polysomes were identified in STED images by visual inspection based on size ((**J**) RPL26: i, 0.32 µm; ii, 0.33 µm; iii, 0.41 µm; iv, 0.24 µm; v, 0.33 µm; (**K**) S6: i, 0.18 µm; ii, 0.27 µm; iii, 0.23 µm) and shape. Scale bars: 0.5 µm wide, 0.2 µm zoom. (**L**) Representative image of RPL26/S6 colocalization analysis using STED imaging. (**M**) Quantification of RPL26/S6 colocalization using Pearson coefficient. (**N**-**P**) Spatial distribution of Sirt1 synthesis and RPL26 in undivided OT-I CD8$^+$ T cells activated on peptide pulsed APCs by STORM. Representative image (**N**) and relation between number of Sirt1/RPL26 co-localization events (**O**) or RPL26 (**P**) cluster and distance towards the MTOC by Poisson regression. Each dot represents the average number of co-localization events across all analyzed cells. (**Q**, **R**) Spatial distribution of cytosolic c-Myc in undivided OT-I CD8$^+$ T cells activated on peptide-pulsed APCs and treated with Ciliobrevin D for the last hour of activation. Representative SoRa image, cytosolic c-Myc is visualized by masking nuclear c-Myc based on Hoechst (**Q**). Scale bar: 2 µm. Quantification of the distribution of cytosolic c-Myc within the cell (**R**). Each dot represents signal in the proximal or distal half of a cell. A line connects data points from two halves of the same cell. Arrows indicate MTOCs. Compiled from two (**M**, **O**, **P**) or three (**B**, **D**-**F**, **R**) independent experiments. Significance was calculated with Wilcoxon signed-rank test against 0 (**M**) or paired (**B**, **D**, **E**, **R**) *Student's t-test*; ****p<0.0001, ns=not statistically significant.

Figure S4

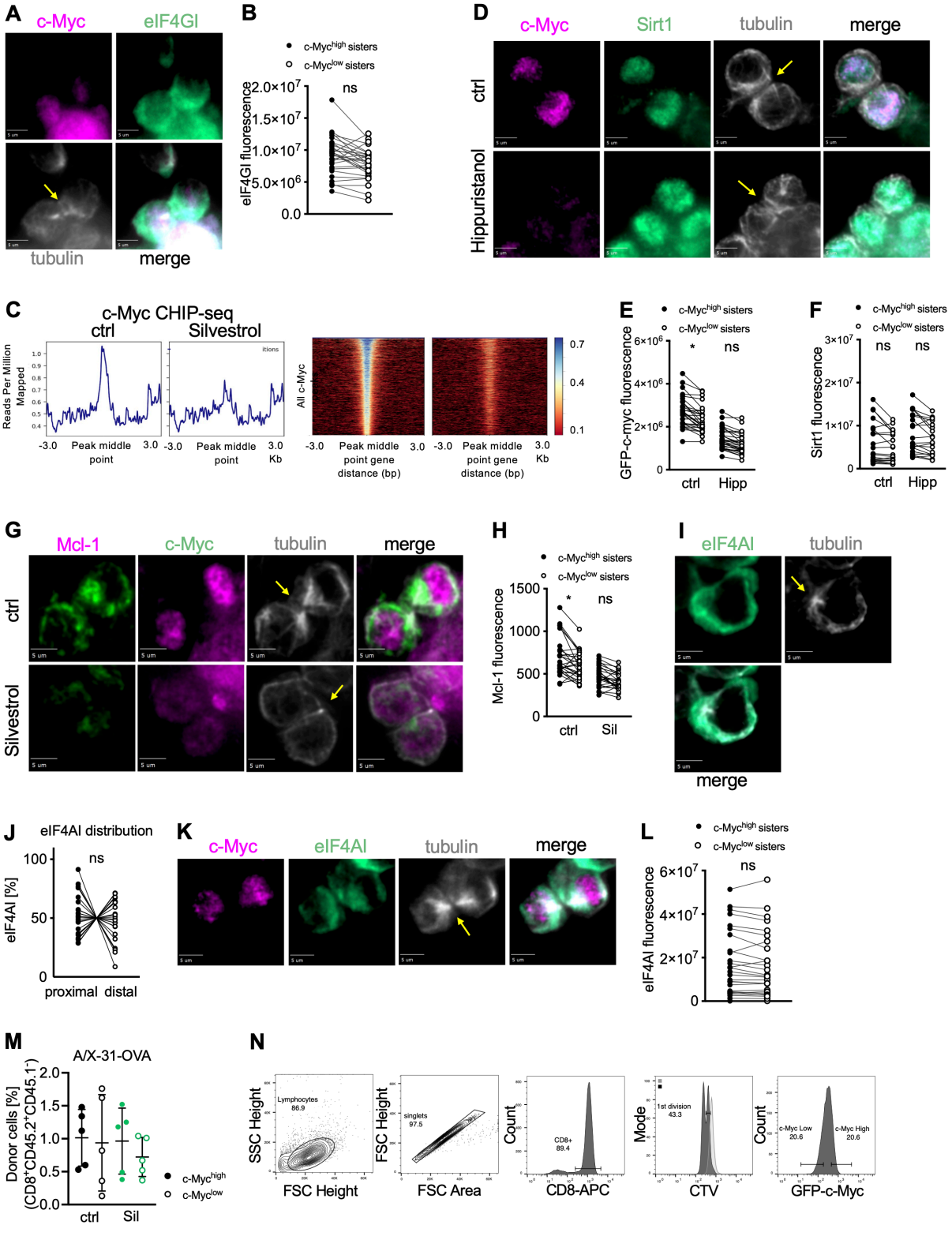
A
c-Myc
eIF4GI
tubulin
merge
B
c-Myc^high sisters
c-Myc^low sisters
ns
eIF4GI fluorescence
2.0×10^7
1.5×10^7
1.0×10^7
5.0×10^6
0.0
D
c-Myc
Sirt1
tubulin
merge
ctrl
Hippuristanol
C
c-Myc CHIP-seq
ctrl
Silvestrol
Reads Per Million Mapped
All c-Myc
-3.0
Peak middle point
3.0
Kb
Peak middle point gene distance (bp)
0.7
0.4
0.1
E
c-Myc^high sisters
c-Myc^low sisters
GFP-c-myc fluorescence
6×10^6
4×10^6
2×10^6
0
*
ns
ctrl
Hipp
F
c-Myc^high sisters
c-Myc^low sisters
Sirt1 fluorescence
3×10^7
2×10^7
1×10^7
0
ns
ctrl
Hipp
G
Mcl-1
c-Myc
tubulin
merge
ctrl
Silvestrol
5 um
H
c-Myc^high sisters
c-Myc^low sisters
Mcl-1 fluorescence
1500
1000
500
0
*
ns
ctrl
Sil
I
eIF4AI
tubulin
merge
J
eIF4AI distribution
eIF4AI [%]
100
50
0
ns
proximal
distal
K
c-Myc
eIF4AI
tubulin
merge
L
c-Myc^high sisters
c-Myc^low sisters
eIF4AI fluorescence
6×10^7
4×10^7
2×10^7
0
ns
M
A/X-31-OVA
Donor cells [%]
(CD8+CD45.2+CD45.1-)
2.0
1.5
1.0
0.5
0.0
c-Myc^high
c-Myc^low
ctrl
Sil
N
SSC Height
FSC Height
Lymphocytes
86.9
FSC Height
FSC Area
singlets
97.5
Count
CD8+
89.4
CD8-APC
Mode
1st division
43.3
CTV
Count
c-Myc Low
20.6
c-Myc High
20.6
GFP-c-Myc

Figure S4. Inhibition of eIF4A at the time of first division promotes memory-like function. Related to Figure 4.

(**A**) Representative images of conjoined sister OT-I GFP-c-Myc $CD8^+$ T cells activated for 28 h on peptide-pulsed APCs. Scale bar: 5 µm. (**B**) Quantification of sum fluorescence intensity of eIF4GI in conjoined sister cells. Each dot represents one cell, data points of sister cells are connected by a line. (**C**) CHIP-seq analysis of c-Myc. Average plots (left) and heatmaps (right). (**D**) Representative images of conjoined daughter OT-I GFP-c-Myc $CD8^+$ T cells activated for 28 h on peptide-pulsed APCs and treated with Hippuristanol for the last hour of activation. Scale bar: 5 µm. (**E**, **F**) Quantification of sum fluorescence intensity of GFP-c-Myc (**E**) or Sirt1 (**F**) in conjoined sister cells. Each dot represents one cell, data points of sister cells are connected by a line. (**G**) Representative images of conjoined daughter OT-I GFP-c-Myc $CD8^+$ T cells activated for 28 h on peptide-pulsed APCs and treated with Silvestrol for the last hour of activation. Scale bar: 5 µm. (**H**) Quantification of mean fluorescence intensity of Mcl-1 in conjoined sister cells. Each dot represents one cell, data points of sister cells are connected by a line. (**I**) Representative images of undivided OT-I $CD8^+$ T cells activated on APCs. Scale bar: 5 µm. (**J**) Quantification of the distribution of eIF4A1 signal within the cell. Each dot represents signal in the proximal or distal half of a cell. A line connects data points from two halves of the same cell. (**K**) Representative images of conjoined daughter OT-I GFP-c-Myc $CD8^+$ T cells activated for 28 h on peptide-pulsed APCs. Scale bar: 5 µm. (**L**) Quantification of sum fluorescence intensity of eIF4A1 in conjoined sister cells. Each dot represents one cell, data points of sister cells are connected by a line. (**M**) Frequency of OT-I GFP-c-Myc $CD8^+$ donor cells (congenic wild type recipients) in peripheral blood on day 9 after A/X-31-OVA infection. Each dot represents a recipient animal, n=5; mean +/- SD. (**N**) Sorting strategy corresponding to Fig. 4H, I. Arrows indicate MTOCs and tubulin bridges. Compiled from two (**F**) or three (**B**, **E**, **H**, **J**, **L**) independent experiments. Significance was calculated with paired *Student's t-test* (**B, J, L**) or ANOVA (**E**, **F, H**); *p<0.05, ns=not statistically significant.

Figure S5

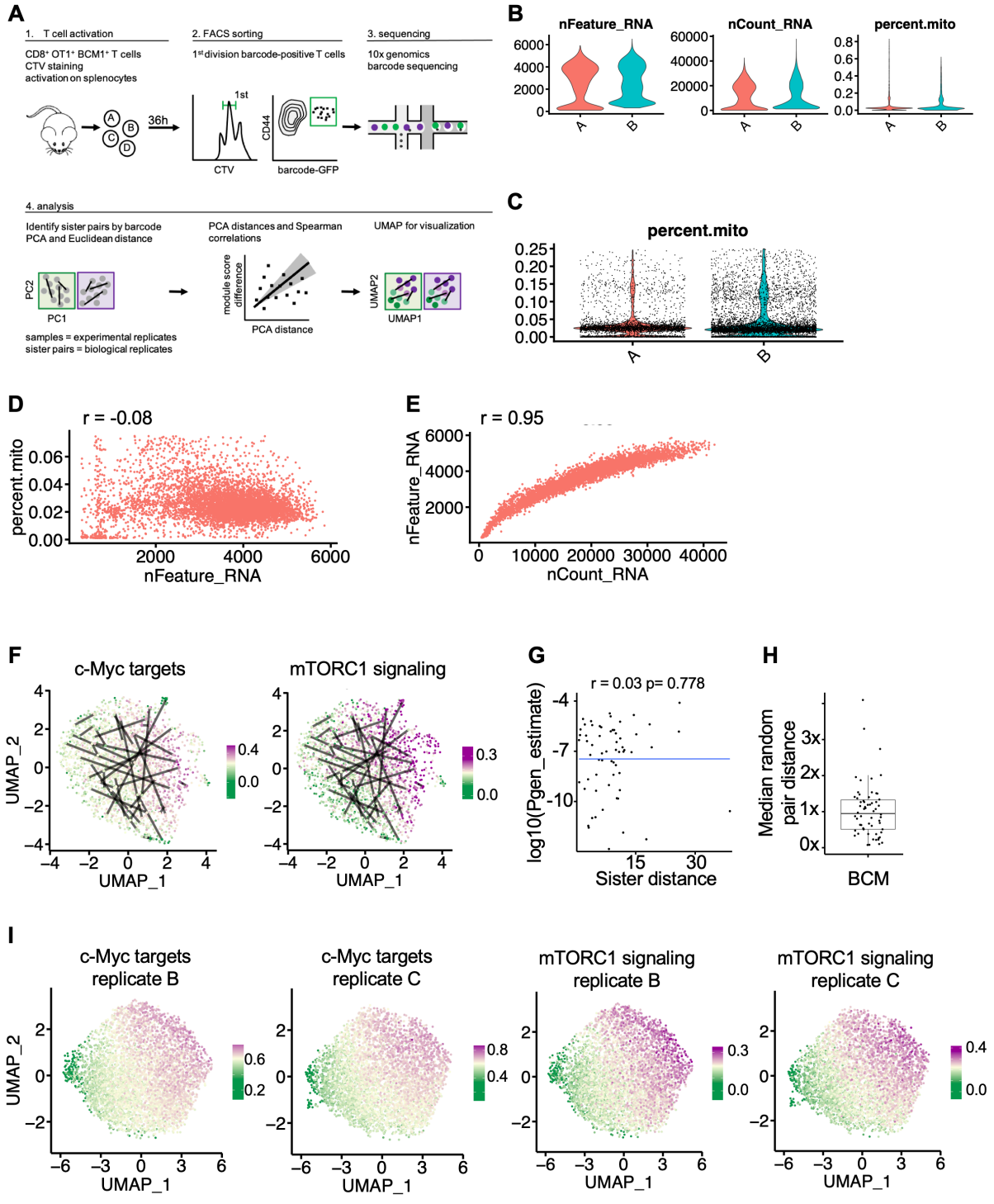
A
1. T cell activation
CD8+ OT1+ BCM1+ T cells
CTV staining
activation on splenocytes
36h
2. FACS sorting
1st division barcode-positive T cells
1st
CTV
CD44
barcode-GFP
3. sequencing
10x genomics
barcode sequencing
4. analysis
Identify sister pairs by barcode
PCA and Euclidean distance
PC2
PC1
samples = experimental replicates
sister pairs = biological replicates
PCA distances and Spearman correlations
module score difference
PCA distance
UMAP for visualization
UMAP2
UMAP1
B
nFeature_RNA
nCount_RNA
percent.mito
C
percent.mito
D
r = -0.08
percent.mito
nFeature_RNA
E
r = 0.95
nFeature_RNA
nCount_RNA
F
c-Myc targets
mTORC1 signaling
UMAP_2
UMAP_1
G
r = 0.03 p= 0.778
log10(Pgen_estimate)
Sister distance
H
Median random pair distance
BCM
I
c-Myc targets replicate B
c-Myc targets replicate C
mTORC1 signaling replicate B
mTORC1 signaling replicate C
UMAP_2
UMAP_1

Figure S5. Transcriptional heterogeneity in sister cells is established as early as the first division. Related to Figure 5.

(**A**) Experimental and analytical approaches to assess transcriptional heterogeneity of first division OT-I BCM $CD8^+$ T sister cells. (**B**) Violin plots representing standard quality control metrics of single cells from two experimental barcode model replicates before filtering out problematic cells. nFeature = the number of genes detected, nCount = the number of unique RNA molecules detected, and percent.mito = the ratio of expression owed to mitochondrial genes versus all other genes, in individual cells. (**C**) Violin plots of the same replicates in (B), with values above 0.25 excluded. Dots represent individual cells before filtering out problematic cells. (**D**, **E**) After filtering, cells exhibit expected relationships between standard quality control metrics, as assessed by Pearson correlations. (**F**) UMAP plots representing single-cell gene expression obtained from barcode experiment replicate B, as described in Fig. 5A. Lines connect putative sister cells. Color gradient corresponds to specific gene set modules scores, where the gradient midpoint (light yellow) is set to the median module score. (**G**) Dot plot depicting the lack of a significant Spearman correlation between pairwise Euclidean PCA distance and barcode-specific probabilities of generation (P_{gen}) for putative sister cell pairs. (**H**) Visualization of sister pair transcriptional differences contextualized by the transcriptional heterogeneity within the entire experiment. Y-axis represents cell-cell PCA distances relative to the median distance between randomly selected pairs. Each point represents a putative sister-cell pair. A value of zero represents identical sister pairs, and a value of 1 represents the median distance between randomly selected pairs. (**I**) UMAP plots representing single-cell gene expression of first-division T cells obtained from replicates B and C of three independent in vivo experiments, otherwise presented as described in (**F**). Additional replicates are presented in Fig. 5.